

SLAC-PUB-4771
LBL-26186
January 1989
E

SEARCHES FOR NON-MINIMAL HIGGS BOSONS FROM A VIRTUAL Z DECAYING INTO A MUON PAIR AT PEP*

S. Komamiya,⁽¹⁾ C. Fordham,⁽¹⁾ G. Abrams,⁽²⁾ C. E. Adolphsen,⁽³⁾ C. Akerlof,⁽⁴⁾
J. P. Alexander,^{(1),(h)} M. Alvarez,^{(5),(a)} D. Amidei,^{(2),(f)} A. R. Baden,^{(2),(m)} J. Ballam,⁽¹⁾
B. C. Barish,⁽⁶⁾ T. Barklow,⁽¹⁾ B. A. Barnett,⁽⁷⁾ J. Bartelt,⁽¹⁾ D. Blockus,⁽⁸⁾
G. Bonvicini,⁽⁴⁾ A. Boyarski,⁽¹⁾ J. Boyer,⁽²⁾ B. Brabson,⁽⁸⁾ A. Breakstone,⁽⁹⁾
J. M. Brom,^{(8),(i)} F. Bulos,⁽¹⁾ P. R. Burchat,⁽³⁾ D. L. Burke,⁽¹⁾ F. Butler,^{(2),(t)}
F. Calvino,^{(5),(d)} R. J. Cence,⁽⁹⁾ J. Chapman,⁽⁴⁾ D. Cords,⁽¹⁾ D. P. Coupal,⁽¹⁾
H. C. DeStaeler,⁽¹⁾ D. E. Dorfan,⁽³⁾ J. M. Dorfan,⁽¹⁾ P. S. Drell,^{(2),(h)} G. J. Feldman,⁽¹⁾
E. Fernandez,^{(5),(a)} R. C. Field,⁽¹⁾ W. T. Ford,⁽⁵⁾ R. Frey,⁽⁴⁾ D. Fujino,⁽¹⁾ K. K. Gan,⁽¹⁾
G. Gidal,⁽²⁾ L. Gladney,^{(1),(u)} T. Glanzman,⁽¹⁾ M. S. Gold,⁽²⁾ G. Goldhaber,⁽²⁾
L. Golding,^{(2),(y)} A. Green,^{(1),(s)} P. Grosse-Wiesmann,⁽¹⁾ J. Haggerty,^{(2),(b)}
G. Hanson,⁽¹⁾ R. Harr,⁽²⁾ F. A. Harris,⁽⁹⁾ C. M. Hawkes,⁽⁶⁾ K. Hayes,⁽¹⁾
D. Herrup,^{(2),(k)} C. A. Heusch,⁽³⁾ T. Himel,⁽¹⁾ M. Hoenk,⁽⁶⁾ R. J. Hollebeek,^{(1),(u)}
D. Hutchinson,⁽¹⁾ J. Hylen,⁽⁷⁾ W. R. Innes,⁽¹⁾ M. Jaffre,^{(2),(o)} J. A. Jaros,⁽¹⁾
I. Juricic,^{(2),(g)} J. A. Kadyk,⁽²⁾ D. Karlen,^{(1),(c)} J. Kent,⁽³⁾ S. R. Klein,⁽¹⁾
A. Koide,^{(9),(k)} W. Koska,⁽⁴⁾ W. Kozanecki,⁽¹⁾ A. J. Lankford,⁽¹⁾ R. R. Larsen,⁽¹⁾
B. W. LeClaire,⁽¹⁾ M. E. Levi,⁽²⁾ Z. Li,⁽⁶⁾ A. M. Litke,⁽³⁾ N. S. Lockyer,^{(1),(u)}
V. Lüth,⁽¹⁾ C. Matteuzzi,^{(1),(e)} J. A. J. Matthews,⁽⁷⁾ D. I. Meyer,⁽⁴⁾ B. D. Milliken,⁽⁶⁾
K. C. Moffett,⁽¹⁾ L. Müller,^{(1),(p)} J. Nash,⁽¹⁾ M. E. Nelson,⁽⁶⁾ D. Nitz,⁽⁴⁾
H. Ogren,⁽⁸⁾ R. A. Ong,^{(1),(f)} K. F. O'Shaughnessy,⁽¹⁾ S. I. Parker,⁽⁹⁾ C. Peck,⁽⁶⁾
A. Petersen,^{(1),(w)} M. Petradza,⁽⁴⁾ F. C. Porter,⁽⁶⁾ P. Rankin,⁽⁵⁾ B. Richter,⁽¹⁾
K. Riles,⁽¹⁾ P. C. Rowson,^{(2),(g)} D. R. Rust,⁽⁸⁾ H. F. W. Sadrozinski,⁽³⁾ T. Schaad,^{(10),(l)}
T. L. Schalk,⁽³⁾ H. Schellman,^{(2),(k)} W. B. Schmidke,⁽²⁾ A. S. Schwarz,^{(3),(r)}
A. Seiden,⁽³⁾ P. D. Sheldon,^{(2),(n)} J. G. Smith,⁽⁵⁾ A. Snyder,⁽⁸⁾ E. Soderstrom,⁽⁶⁾
D. P. Stoker,⁽⁷⁾ R. Stroynowski,⁽⁶⁾ R. Thun,⁽⁴⁾ G. H. Trilling,⁽²⁾ R. Tschirhart,^{(4),(v)}
C. de la Vaissiere,^{(2),(q)} R. Van Kooten,⁽¹⁾ H. Veltman,^{(4),(z)} P. Voruganti,⁽¹⁾
S. R. Wagner,⁽⁵⁾ P. Weber,⁽⁵⁾ A. J. Weinstein,⁽⁶⁾ A. J. Weir,⁽⁶⁾ S. Weisz,^{(3),(e)}
S. L. White,^{(5),(x)} E. Wicklund,⁽⁶⁾ D. R. Wood,^{(2),(e)} D. Y. Wu,⁽⁶⁾ and J. M. Yelton^{(1),(j)}

Submitted to *Physical Review D*

* This work was supported in part by Department of Energy contracts DE-AC03-81ER40050 (CIT), DE-AM03-76SF00010 (UCSC), DE-AC02-86ER40253 (Colorado), DE-AC03-83ER40103 (Hawaii), DE-AC02-84ER40125 (Indiana), DE-AC03-76SF00098 (LBL), DE-AC02-84ER40125 (Michigan), and DE-AC03-76SF00515 (SLAC), and by the National Science Foundation (Johns Hopkins).

- (1) *Stanford Linear Accelerator Center, Stanford University, Stanford, California 94309*
(2) *Lawrence Berkeley Laboratory and Department of Physics,
University of California, Berkeley, California 94720*
(3) *University of California, Santa Cruz, California 95064*
(4) *University of Michigan, Ann Arbor, Michigan 48109*
(5) *University of Colorado, Boulder, Colorado 80309*
(6) *California Institute of Technology, Pasadena, California 91125*
(7) *Johns Hopkins University, Baltimore, Maryland 21218*
(8) *Indiana University, Bloomington, Indiana 47405*
(9) *University of Hawaii, Honolulu, Hawaii 96822*
(10) *Harvard University, Cambridge, Massachusetts 02138*

-
- (a) Present address: Universidad Autónoma de Barcelona, Bellaterra, Spain
(b) Present address: Brookhaven National Laboratory, Upton, NY 11973
(c) Present address: Carleton University, Ottawa, Ontario, Canada, K1S 5B6
(d) Present address: Universitat Politecnica de Catalunya, ETSEIB-DEN Barcelona, Spain
(e) Present address: CERN, CH-1211, Genève 23, Switzerland
(f) Present address: University of Chicago, Chicago, IL 60637
(g) Present address: Columbia University, New York, NY 10027
(h) Present address: Cornell University, Ithaca, NY 14853
(i) Present address: Centre de Recherches Nucléaires, F-67037 Strasbourg, France
(j) Present address: University of Florida, Gainsville, FL 32611
(k) Present address: Fermilab, Batavia, IL 60510
(l) Present address: Université de Genève, CH-1211, Genève 4, Switzerland
(m) Present address: Harvard University, Cambridge, MA 02138
(n) Present address: University of Illinois, Urbana, IL 61801
(o) Present address: Laboratoire de l'Accélérateur Linéaire, F-91405 Orsay, France
(p) Present address: Lab. für Hochenergie Physik Bern, CH-3012 Bern, Switzerland
(q) Present address: Univ. Pierre Marie Curie, F-75230, Paris, France
(r) Present address: Max-Planck Institut, München, F. R. Germany
(s) Present address: O'Conner and Associates, Chicago, IL 60604
(t) Present address: University of Oklahoma, Norman, OK 73019
(u) Present address: University of Pennsylvania, Philadelphia, PA 19104
(v) Present address: Princeton University, Physics Department, Princeton, NJ 08544
(w) Present address: SCS, Hamburg, F. R. Germany
(x) Present address: University of Tennessee, Knoxville, TN 37996
(y) Present address: Therma-Wave Corporation, Fremont, CA 94539
(z) Present address: University of California, Berkeley, CA 94720
(α) Present address: Vista Research Inc., P. O. Box 998, Mountain View, CA 94042

ABSTRACT

Non-minimal neutral Higgs bosons decaying into a muon pair were searched for using the Mark II detector at the PEP e^+e^- collider at $\sqrt{s} = 29$ GeV. A neutral scalar Higgs boson H_s^0 can be produced accompanied by a pseudoscalar neutral Higgs boson H_p^0 via a virtual Z^0 . If the mass of one of the Higgs bosons is between the muon pair threshold and the kaon pair threshold, it may decay predominantly into a muon pair. We looked for muon pair + jet(s) [$e^+e^- \rightarrow H_s^0 H_p^0 \rightarrow \mu^+\mu^- + q\bar{q}(\tau^+\tau^-)$] and three muon pair [$e^+e^- \rightarrow H_s^0 H_p^0 \rightarrow 3(H_p^0) \rightarrow 3(\mu^+\mu^-)$] topologies. We found no evidence for these signals above the known background level, and we obtained limits on $\Gamma(Z^0 \rightarrow H_s^0 H_p^0)$ as a function of the Higgs boson masses.

1. Introduction: Two Higgs Doublet Models

We have searched for the production of light Higgs bosons decaying into muon pairs for a Higgs sector consisting of more than one doublet.

In the standard model, the Higgs sector is necessary to give mass to the weak gauge bosons as well as to the quarks and leptons. The Higgs boson is also necessary in order to prevent the cross section from violating unitarity for some fundamental processes (e.g. $W^+W^- \rightarrow W^+W^-$, $e^+e^- \rightarrow W^+W^-$, etc.).

Only one physical scalar Higgs boson is expected to exist in the minimal Higgs sector. If the Higgs sector is non-minimal, there will be additional physical neutral and charged Higgs bosons. Since the ρ parameter ($\rho = \frac{M_W^2}{M_Z^2 \cos^2 \theta_w}$) is experimentally consistent with unity^[1], the structure of the Higgs multiplet is probably an SU(2) doublet (or singlet)^[2]. At least two Higgs doublets are necessary for most supersymmetric models^[3] and visible axion models.^[4] Such an extension of the standard Higgs sector adds another SU(2) Higgs doublet:

$$\phi_1 = \begin{pmatrix} \phi_1^+ \\ \phi_1^0 \end{pmatrix}, \quad \phi_2 = \begin{pmatrix} \phi_2^+ \\ \phi_2^0 \end{pmatrix},$$

where ϕ_1^+ , ϕ_1^0 , ϕ_2^+ and ϕ_2^0 are complex fields. For these models, there are three physical neutral Higgs bosons (H_1^0 , H_2^0 , H_3^0) and two charged Higgs bosons (H^+ and H^-). In the case of the neutral non-minimal Higgs bosons, H_3^0 is a pseudoscalar and the other two are scalars, if their parity is defined through their couplings with fermions. To be more precise, H_3^0 is a CP -odd state and the other neutrals (H_1^0 and H_2^0) are CP -even states, if CP is conserved at tree level.^{[5][6]}

In this report, H_s^0 denotes a scalar Higgs boson and H_p^0 denotes a pseudoscalar. We also use the notation H_i^0 and H_j^0 for the two Higgs bosons, where H_i^0 is assumed to decay into $\mu^+\mu^-$ regardless of its CP state, and H_j^0 has opposite CP to H_i^0 .

2. Associated Production and Decay of Scalar and Pseudoscalar Neutral Higgs Bosons

A scalar Higgs boson associated with a pseudoscalar can be produced from a virtual Z^0 in e^+e^- annihilation via the process $e^+e^- \rightarrow Z^0 \rightarrow H_s^0 H_p^0$ ($H_s^0 = H_1^0$ or H_2^0 , $H_p^0 = H_3^0$) (see Fig. 1a). The total cross section for this process is

$$\sigma = \frac{1}{2} \sigma_{\nu_\mu \bar{\nu}_\mu} \cdot \bar{\beta}^3 \cos^2(a - b) \quad (1)$$

where $\bar{\beta} = \frac{2P_{CM}}{\sqrt{s}} = \sqrt{[s - (M_s + M_p)^2][s - (M_s - M_p)^2]}/s$, $\sigma_{\nu_\mu \bar{\nu}_\mu}$ is the cross section for the decay of the virtual Z^0 into two muon neutrinos, and a and b are mixing angles.^{[7][8]} The angular distribution in the center-of-mass system is $d\sigma/d\Omega \propto \sin^2 \theta$.

The interactions of Higgs bosons with fermions can be determined from the fermion mass term in the Lagrangian. The couplings differ from model to model and depend on how each Higgs field contributes to each fermion mass. The important constraint on the Higgs couplings is that flavor changing neutral currents (FCNC) cannot be induced by the neutral Higgs bosons. Therefore, the condition is imposed that each fermion type couple with only one of the two Higgs doublets.^{[9][10]}

The decay modes of the scalar and the pseudoscalar Higgs bosons depend on their masses and mixing angles. In principle, they will decay into the heaviest available fermion pair: $H_i^0 \rightarrow f\bar{f}$ (Fig. 1b). If the scalar mass is more than two times the pseudoscalar mass, $H_s^0 \rightarrow H_p^0 H_p^0$ is the dominant decay mode (Fig. 1c) unless this is suppressed by the Higgs mixing.^[11]

Limits on some non-minimal Higgs masses and couplings already exist. Some parameter ranges are excluded by searches for the standard-model Higgs boson. Recently, CLEO has searched for B -meson decay into a K meson plus a neutral Higgs boson, for the Higgs boson decay modes $H^0 \rightarrow \mu^+\mu^-$, $\pi^+\pi^-$, $K\bar{K}$, $K\bar{K}^*$, $K^*\bar{K}$ and $K^*\bar{K}^*$.^[12] They exclude the standard Higgs boson from mass ranges between 0.3 and 3.0 GeV and between 3.2 and 3.6 GeV. Chivukula and Manohar^[13] summarized the light standard model Higgs boson searches in K and B decay and

concluded that the standard-model Higgs boson has been excluded up to a mass of $2M_\tau$ if the number of generations is three, and up to 0.36 GeV independent of the number of generations. The CUSB II group has searched for $\Upsilon \rightarrow H^0\gamma$ and excluded the standard Higgs boson mass from the region between the muon pair threshold and 5.0 GeV.^[14] These limits also constrain the non-minimal Higgs boson mass. However, since the non-minimal Higgs boson couplings to the b quark and other fermions are model dependent, their masses in these regions are not excluded in a model independent way.

Searches for non-minimal Higgs bosons from virtual Z^0 's have been performed at PEP and PETRA. Glashow and Manohar^[15] have suggested that the UA1 mono-jet events^[16] can result from an anomalous decay of the Z^0 into two different Higgs bosons ($H_p^0 H_s^0$), where H_s^0 is very light ($< 2M_\mu$) and hence stable. In the beginning of 1985, negative results on these monojets were reported by HRS,^[17] MAC,^[18] and Mark-II^[19] at PEP, and by CELLO^[20] and JADE^[21] at PETRA.

Another topology was studied by JADE,^[22] motivated by the 1.7 MeV axion interpretation^{[23][24]} of the correlated GSI positron and electron kinetic energy peaks at about 0.3-0.4 MeV.^[25] At PETRA, this axion (H_p^0) can be produced accompanied by a scalar Higgs boson via a virtual Z^0 .^[26] Since the scalar is very much heavier than the axion, the H_s^0 decays immediately into $H_p^0 H_p^0$, and all three axions decay into e^+e^- with long decay length. For the model by Peccei, et al.,^[23] scalar masses up to about 5 GeV are excluded with 90% C.L.^[22] Note, however, that these models are now excluded by the combined experimental results from rare pion decays^[27] and beam dump experiments,^[28] independent of the scalar mass.

The analysis described in this paper is an extension of the above searches for the non-minimal Higgs boson to the mass region above the muon pair threshold. If the mass of the lighter neutral Higgs boson (H_i^0) is between $2M_\mu$ and $2M_K$, it could decay into a muon pair with a large branching fraction. Even above the kaon pair threshold and below the tau pair threshold, the branching fraction into a muon pair can be fairly large, since the Higgs boson couples to the current quark masses, and

the lightest Higgs boson might not couple to quarks. Scalar Higgs bosons also decay into $\pi^+\pi^-$ through two gluons via a heavy quark loop. For the standard Higgs boson this branching fraction is estimated to be large;^[29] therefore the branching fraction for $H^0 \rightarrow \mu^+\mu^-$ would be small for $2M_\pi < M_{H^0} < 2M_K$. For non-minimal neutral Higgs bosons, the branching fraction depends on the couplings and can be larger. Particularly for pseudoscalar Higgs bosons, the $H_p^0 \rightarrow \pi^+\pi^-$ or K^+K^- mode is highly suppressed by parity, and the $H_p^0 \rightarrow \pi^+\pi^-\pi^0$ and $H_p^0 \rightarrow \gamma\gamma$ modes are suppressed for the same reason that $\eta \rightarrow \pi^+\pi^-\pi^0$ and $\eta \rightarrow \gamma\gamma$ decays occur only via the electromagnetic interaction.^[30]

We searched for a light non-minimal neutral Higgs boson decaying into a $\mu^+\mu^-$ pair, accompanied by a heavier neutral Higgs boson. There are two cases which are characterized by the major decay mode of the heavier Higgs boson. If the heavier Higgs boson (H_j^0) decays into a heavy fermion pair, the final states are $\mu^+\mu^- b\bar{b}$, $\mu^+\mu^- c\bar{c}$, $\mu^+\mu^- \tau^+\tau^-$, etc. (Case I). On the other hand, if the heavier scalar Higgs boson (H_s^0) decays into two H_p^0 's and all three H_p^0 decay into muon pairs, the final state is six muons (Case II). The detector used for the search is described in Chapter 3; the analyses for the two cases are described in Chapters 4 and 5.

3. Apparatus

The data analyzed here were acquired by two different configurations of the Mark II detector at PEP. The center-of-mass energy for all of the data was 29 GeV. An integrated luminosity of 210 pb^{-1} was taken with the first configuration of the detector, which has been described extensively elsewhere.^[31] The components of the detector most important to this analysis were the tracking chambers and the muon system. Charged particle tracks were measured by a 16-layer cylindrical drift chamber and a high-resolution vertex drift chamber in a 2.3-kG axial magnetic field. This combination gave a vertex-constrained momentum resolution of $(\frac{\sigma_p}{p})^2 = (0.025)^2 + (0.011p)^2$ (p in GeV). The drift chamber did not have multiple-hit readout capability.

The muon system consisted of planes at the top and bottom and both sides of the detector, each containing four layers of iron absorber followed by proportional tubes. The muon system covered 45% of the solid angle, and any muons outside that solid angle were not identified.

The electromagnetic calorimeters and time-of-flight system (TOF) were used in background elimination. The electromagnetic calorimeter system consisted of eight modules in an octagonal array outside the magnet coil. The modules consisted of 37 layers of 2 mm thick lead planes and 3 mm thick liquid argon gaps. Details of the liquid argon system are described elsewhere.^[32] The time-of-flight system consisted of 48 plastic scintillators at 1.51 m from the vertex; its RMS timing resolution was 350 ps.

In preparation for the change to SLC running, the Mark II detector was upgraded.^[33] This upgraded detector was operated at PEP briefly and accumulated approximately 15 pb^{-1} of data with the muon system on. The changes to the detector were a new 72 layer drift chamber,^[34] a new vertex chamber,^[35] a new time-of-flight system, new endcap calorimeters,^[36] and a coil capable of fields up to 5.0 kG. The vertex-constrained momentum resolution improved to $(\frac{\sigma_p}{p})^2 = (0.014)^2 + (0.003p)^2$. The new drift chamber has multiple-hit readout and pulse digitization capabilities, which improves its two-track separation over that of the old drift chamber. For the new time-of-flight system, $\sigma_{TOF} = 221 \text{ ps}$.

4. Analysis (Case I : $e^+e^- \rightarrow H_s^0 H_p^0 \rightarrow \mu^+\mu^- + f\bar{f}$)

4.1. EVENT SELECTION

The signature for these events is an isolated muon pair with small opening angle. The event selection was started from $5.85 \cdot 10^5$ events on the data summary tapes (DST's). The data reduction cuts made before writing to these tapes which affected this analysis were mainly the following two cuts:

- (DST1) The visible energy (charged and photon) of an event was larger than $0.25\sqrt{s}$ ($0.15\sqrt{s}$ for data taken with the upgraded detector).
- (DST2) The visible charged energy of an event was larger than $0.125\sqrt{s}$ ($0.075\sqrt{s}$ for data taken with the upgraded detector).

The integrated luminosity corresponding to the data we analysed is 225 pb^{-1} . The experimental selection criteria for these events are the following:

- (1) The total charged multiplicity of the event is greater than or equal to four.
- (2) There is at least one oppositely charged pair (i, j) of tracks with opening angle ψ_{ij} satisfying $\psi_{ij} < 38^\circ$. This cut is optimized so that the muon pairs whose invariant mass is smaller than $2M_\tau$ can be detected efficiently. Hence Higgs bosons with mass between $2M_K$ and $2M_\tau$ may also decay into muon pairs with a reasonably large branching fraction and be detected.
- (3) The polar angles (θ_i and θ_j) of both particles in the pair should satisfy the condition $|\cos \theta_i| < 0.8$ and $|\cos \theta_j| < 0.8$. This cut naturally enriches the Higgs signal since the angular distribution of the Higgs boson peaks at $\theta = 90^\circ$ ($d\sigma/d \cos \theta \propto \sin^2 \theta$).
- (4) The momenta of the two charged particles are : $|\vec{p}_i| > 1.8 \text{ GeV}$, $|\vec{p}_j| > 1.8 \text{ GeV}$.
- (5) Except for the particles i and j , no charged particles ($p > 0.2 \text{ GeV}$) are within a 60 degree cone from the momentum sum $(\vec{p}_i + \vec{p}_j)$ of the pair. The total photon energy within the 60 degree cone is less than 1.0 GeV.
- (6) Out of time cosmic muons, which are reconstructed as two parallel tracks in the chamber, are rejected by using the TOF counter information. The event is rejected if both tracks do not have a hit in a TOF counter and if the timing is far from nominal.

After these topology cuts, 945 events survived. Since these cuts alone were not enough to isolate the signal, the following lepton identification cuts were added.

- (7) Both tracks must be identified as good muons: all four layers of the muon tubes must have hits within 3σ of the track extrapolation from the central drift chamber, taking into account fit and multiple scattering errors. In order to hit the muon system, the polar angle of the track must satisfy $|\cos \theta| < 0.45$.
- (8) Finally, $e^+e^-\mu^+\mu^-$ events due to pure QED processes are rejected by removing the following events:
 - (a) Events with charged multiplicity equal to four and with at least one identified electron. An identified electron was defined as a track in the liquid argon fiducial volume which had $\frac{E_{min}}{p} > 0.8$, where E_{min} is defined elsewhere.^[37] The electron cut was loose in order to eliminate as many QED events as possible.
 - (b) Events with at least one identified electron and with no reconstructed charged pions, which are defined as charged tracks which are neither identified electrons nor identified muons.

The detection efficiency for the events is obtained by running the analysis program on data generated by a Monte Carlo calculation with a full detector simulation. For opening angles greater than 10° , the detection efficiency is typically 15% to 20%. It does not depend much on the lighter Higgs boson mass unless the mass is very close to the muon pair threshold. The efficiency for resolving the two muon tracks decreases with decreasing opening angle. If one considers angles less than 10° , for the old Mark II chamber, the efficiency decreases to 7% at $M_{H^0} = 0.22$ GeV; for the upgrade Mark II drift chamber, the efficiency is 13%, significantly better than for the old drift chamber.

After all the cuts (1-8) three events survive. Measured parameters for the three surviving events are listed in Table 1, where $m_{\mu^+\mu^-}^2$ is the squared invariant mass for the muon pair, and m_{recoil}^2 is the squared invariant mass of the particles

recoiling against the muon pair:

$$m_{recoil}^2 = (\sqrt{s} - \sqrt{(\vec{p}_{\mu 1})^2 + M_\mu^2} - \sqrt{(\vec{p}_{\mu 2})^2 + M_\mu^2})^2 - (\vec{p}_{\mu 1} + \vec{p}_{\mu 2})^2.$$

Table 1
Parameters of the Surviving Three Events

Event	(A)	(B)	(C)
$ \vec{p}_{\mu+} $ GeV	5.55 ± 0.28	8.52 ± 0.58	11.75 ± 0.92
$ \vec{p}_{\mu-} $ GeV	2.43 ± 0.09	5.19 ± 0.24	2.90 ± 0.12
$m_{\mu+\mu-}^2$ GeV 2	0.266 ± 0.0164	0.111 ± 0.0131	0.836 ± 0.0722
m_{recoil}^2 GeV 2	$378. \pm 17.1$	45.6 ± 36.4	-7.35 ± 53.7
visible tracks	7	4	5
E_{vis}/\sqrt{s}	0.519	0.963	0.966

4.2. BACKGROUND ESTIMATION

The most obvious sources of background are the two-photon processes, where one of the virtual photons is converted into a muon pair and the other into a quark or tau pair (see Fig. 1e). The expected number of background events from these processes after the cuts is 0.92 ± 0.14 , estimated using the Berends–Daverveldt–Kleiss Monte Carlo program^[38] and incorporating the hadronic fragmentation of the quark pair by the Lund scheme.

The number of background events due to multihadronic events containing two real muons is estimated by the Monte Carlo calculation. If a B -meson decays into $\mu\nu D$ and the D into a $\mu\nu$ plus a K_L^0 while the \bar{B} -meson decays into hadrons, for example, the event has an isolated pair of oppositely charged muons and no charged hadrons within that hemisphere produced from fragmentation; it would pass the

cuts. Monte Carlo $b\bar{b}$ events were passed through the same analysis chain as the real data. The number of background events thus estimated for this category is 0.72 ± 0.28 .

We estimate the background due to fake muons, namely hadron punch-through or K^\pm - or π^\pm -decays into muons, by using the data and fake muon probabilities. The expected number of background events for the case where only one of the isolated muon pair tracks is a misidentified hadron is estimated by summing the misidentification probability for a hadron into a muon, $P_{h \rightarrow \mu}(\vec{p}_i)$, over all events satisfying all the selection criteria except the muon identification for one of the tracks; instead, the track must be a hadron. There are 9 such events in the whole data sample. The probability $P_{h \rightarrow \mu}(\vec{p}_i)$ is given elsewhere.^[39] The estimated background is 0.08 ± 0.03 . For the case where both muons are misidentified hadrons, the estimated background is

$$\sum P_{h \rightarrow \mu}(\vec{p}_i) P_{h \rightarrow \mu}(\vec{p}_j).$$

The sum is performed over the events surviving all the cuts except the muon identification (cut 7); instead, the both of the pair tracks are categorized as hadrons (each of the two identified neither as an electron nor as a muon). The estimated background is 0.015 ± 0.004 . The error is dominated by the systematic error in the misidentification probability. Therefore the expected number of background events due to misidentified muons is small (about 0.10 events). The summary of the background is listed in Table 2. The total number of background events is estimated to be 1.73 ± 0.32 , while the number of observed events is three. Therefore all of the three events are consistent with background.

Table 2
Comparison of number of background events

Background	expected number
$e^+e^- \rightarrow \mu^+\mu^-q\bar{q}$	0.76 ± 0.14
$e^+e^- \rightarrow \mu^+\mu^-\tau^+\tau^-$	0.15 ± 0.03
$e^+e^- \rightarrow b\bar{b} \rightarrow \mu^+\mu^-X$	0.72 ± 0.28
fake: $\mu^\pm h^\mp \rightarrow \mu^\pm\mu^\mp$	0.08 ± 0.03
fake: $h^+h^- \rightarrow \mu^+\mu^-$	0.02 ± 0.01
total	1.73 ± 0.32

4.3. LIMIT ON THE DECAY WIDTH FOR THE PROCESS $Z^0 \rightarrow H_s^0 H_p^0$

From Equ.(1) the cross section for the process $e^+e^- \rightarrow H_s^0 H_p^0$ via a virtual Z^0 at $\sqrt{s} = 29$ GeV is

$$\sigma = 0.153 \text{ pb} \cdot \bar{\beta}^3 \cos^2(a - b),$$

where $\bar{\beta} = 2p_{H_s^0}/\sqrt{s} = 2p_{H_p^0}/\sqrt{s}$, and a and b are the Higgs mixing angles. The number of events expected for our measured luminosity is $34.4 \bar{\beta}^3 \cos^2(a - b)$.

Fig. 2 shows the expected distribution of events for $m_{\mu\mu}^2$ vs m_{recoil}^2 when $M_{H_s^0} = 0.3$ GeV and $M_{H_p^0} = 5$ GeV. The projection of the distribution onto each axis is also shown in the figure. The surviving three events are indicated in the figure with error bars.

The 90% C.L. upper limit of the number of signal events s_{lim} is obtained by using a likelihood method, taking into account the number of expected background events and its estimated error, the background distribution m_{recoil}^2 vs $m_{\mu\mu}^2$, and the errors in the invariant mass squared ($m_{\mu\mu}^2$ and m_{recoil}^2) in the observed three events. The details of the likelihood function are described in appendix A.

In order to have a somewhat model independent result, the limit is obtained

for the partial width of the Z^0 decay into $H_i^0 + H_j^0$ normalized to the $Z^0 \rightarrow \nu_\mu \bar{\nu}_\mu$ width multiplied by the Higgs branching fraction into a muon pair. Fig. 3a shows the limit as a function of the heavier Higgs mass for the fixed lighter Higgs mass of 0.28 GeV. The excluded region of the relative width for a given mass combination is normalized to the value for a real Z^0 :

$$\frac{\Gamma(Z^0 \rightarrow H_i^0 H_j^0)}{\Gamma(Z^0 \rightarrow \nu_\mu \bar{\nu}_\mu)} Br(H_i^0 \rightarrow \mu^+ \mu^-) > \frac{s_{lim}}{\sigma_{\nu_\mu \bar{\nu}_\mu} \int L dt \epsilon \bar{\beta}^3},$$

where $\sigma_{\nu_\mu \bar{\nu}_\mu}$ is the $\nu_\mu \bar{\nu}_\mu$ cross section at $\sqrt{s} = 29$ GeV, ϵ is the detection efficiency, $\bar{\beta}_o$ is the $\bar{\beta}$ value on the Z^0 peak. This method eliminates the $\bar{\beta}^3$ threshold effect for heavy Higgs bosons at $\sqrt{s} = 29$ GeV so that the limit can be compared with future results at the Z^0 -peak from SLC/LEP.

For the most optimistic case, shown by the "Maximum Width" curve (no reduction of the cross section by the mixing) in Fig.3a, the heavier Higgs boson mass can be excluded up to about 12 GeV with 90 % C.L. for a lighter Higgs boson mass of 0.28 GeV (just below the $\pi^+ \pi^-$ threshold). Fig. 4a shows the excluded region in the $M_{H_i^0} - M_{H_j^0}$ plane if $Br(H_i^0 \rightarrow \mu^+ \mu^-) = 100\%$ and the cross section is maximum (no suppression due to the Higgs mixing). The three dips shown in the figure are due to the surviving three events.

5. Analysis (Case II : $e^+ e^- \rightarrow H_p^0 H_s^0 \rightarrow H_p^0 H_p^0 H_p^0$)

5.1. EVENT SELECTION

The signature of the events we are looking for is three isolated muon pairs with a small opening angle for each pair. The event selection began with the data summary tapes (DST's) as in Case I. We applied a set of simpler experimental cuts for this case:

- (1A) The total charged multiplicity of the event is between five and seven.
- (2A) The total visible charged particle energy of the event exceeds $\sqrt{s}/2$.

- (3A) The event has three or more good muons: all four layers of the muon tubes have hits within 3σ of the track extrapolation from the central drift chamber, taking into account fit and multiple scattering errors.

After all cuts (1A-3A) no events survived. The detection efficiency is about 25 % for $M_{H_p^0} = 0.3$ GeV almost independent of $M_{H_s^0}$ for $M_{H_s^0} < 10$ GeV.

We also tried another set of cuts which do not depend on the muon detector system:

- (1B) The total charged multiplicity of the event is equal to six, with all six charged particles having $p > 0.7$ GeV.
- (2B) The visible charged particle energy (assuming the pion mass for each particle) must exceed 26 GeV.
- (3B) The total missing momentum normalized to the scalar sum of the six momenta must be less than 0.3.
- (4B) There exists a combination of the six prongs such that three oppositely charged particle pairs have invariant masses which coincide to within 0.20 GeV when each pair is allowed to be e^+e^- , $\mu^+\mu^-$, $\pi^+\pi^-$ or K^+K^- . This allows us to find combinations of $e^+e^- + \mu^+\mu^- + \mu^+\mu^-$ etc. The opening angle of the two particles for each pair is less than 90° .

After the cuts (1B-4B) no events survived. The detection efficiency depends on both Higgs boson masses since both masses affect the opening angle between pairs. A small opening angle can cause tracks to be lost due to the limits of double track resolution. The detection efficiency is 22% for $M_{H_p^0} = 0.3$ GeV and $M_{H_s^0} = 5$ GeV, and increases to 25% when $M_{H_s^0}$ increases to 10 GeV. With $M_{H_s^0}$ fixed at 5 GeV, the efficiency increases to 34% for $M_{H_p^0} = 0.5$ GeV and decreases to 11% for $M_{H_p^0} = 0.25$ GeV.

We used the set of cuts (1A-3A or 1B-4B) with larger detection efficiency for each set of Higgs boson masses.

5.2. LIMIT ON THE DECAY WIDTH OF $Z^0 \rightarrow H_s^0 H_p^0$

For the case of $H_s^0 \rightarrow H_p^0 H_p^0$, the limit is obtained using Poisson statistics based on no observed events assuming no expected background. Just as in Fig. 3a, Fig. 3b shows the limit of the partial width of the Z^0 -decay into $H_s^0 + H_p^0$, normalized to the $Z^0 \rightarrow \nu_\mu \bar{\nu}_\mu$ width, as a function of the heavier Higgs boson mass. Fig. 4b shows the excluded region in the $M_{H_s^0}$ - $M_{H_p^0}$ plane if $Br(H_p^0 \rightarrow \mu^+ \mu^-) = 100\%$ and the cross section is maximal (no suppression due to Higgs mixing).

6. Conclusions

We looked for evidence for the associated production of scalar and pseudoscalar neutral Higgs bosons from a virtual Z^0 , where one of the Higgs bosons decays into a muon pair. For the case where $H_s^0 H_p^0 \rightarrow \mu^+ \mu^- f\bar{f}$, three events remain after all the cuts. They are consistent with the expected background from two photon processes and from multihadronic events. No events were found in the search for $H_s^0 H_p^0 \rightarrow H_p^0 H_p^0 H_p^0 \rightarrow 3\mu^+ \mu^-$. Production of non-minimal neutral Higgs bosons and their decay into muon pairs is limited for a mass region between the muon pair threshold and the tau pair threshold. The limits depend on the branching fractions and the degree of suppression of the cross section due to Higgs mixing.

7. Acknowledgements

We would like to thank Howard Haber for many useful discussions.

Appendix A (Likelihood function used for case I)

The likelihood function used to calculate the 90% C.L. limit of number of signal events is a product of three probability functions:

$$\mathcal{L}(s, b) = \mathcal{P}_{Poisson}(s, b) \mathcal{P}_{Bkg}(b) \prod_{n=1}^3 \frac{(s f_n + b g_n)}{(s+b)}.$$

The parameters in the function are number of signal events s and number of background events b after the cuts.

The first function $\mathcal{P}_{Poisson}(s, b)$ is the Poisson distribution of signal plus background events where the observed number is 3 events:

$$\mathcal{P}_{Poisson}(s, b) = \exp(-s - b) \frac{(s+b)^3}{3!}.$$

The second function $\mathcal{P}_{Bkg}(b)$ is the number of background events b assuming a Gaussian distribution:

$$\mathcal{P}_{Bkg}(b) = \frac{1}{\sqrt{2\pi}\sigma_b} \exp\left[-\frac{(b - b_o)^2}{2\sigma_b^2}\right]$$

where b_o is the estimated number of background events ($b_o = 1.73$) and σ_b is its error ($\sigma_b = 0.32$) as listed in Table 2. This function restricts the number of background events, b , to be close to the estimated value, b_o .

The factor $\prod_n \frac{(s f_n + b g_n)}{(s+b)}$ is the likelihood, given n observed events, that they will have particular measured values of $m_{\mu^+ \mu^-}^2$ and m_{recoil}^2 . The functions f and g are the probability distribution of signal and background events in $m_{\mu\mu}^2$ vs m_{recoil}^2 :

$$f_n = f(m_{\mu\mu,n}^2, m_{recoil,n}^2) = \frac{1}{\sqrt{2\pi}\Delta(m_{\mu\mu,n}^2)} \exp\left(-\frac{(m_{\mu\mu,n}^2 - M_{H_i^0}^2)^2}{2\Delta(m_{\mu\mu,n}^2)^2}\right) \\ \cdot \frac{1}{\sqrt{2\pi}\Delta(m_{recoil,n}^2)} \exp\left(-\frac{(m_{recoil,n}^2 - M_{H_j^0}^2)^2}{2\Delta(m_{recoil,n}^2)^2}\right),$$

where $\Delta(m_{\mu\mu,n}^2)$ and $\Delta(m_{recoil,n}^2)$ are the measured errors of $m_{\mu\mu,n}^2$ and $m_{recoil,n}^2$,

respectively, as listed in Table 2, and

$$g_n = g(m_{\mu\mu,n}^2, m_{recoil,n}^2) = \kappa \lambda \exp(\kappa (4M_\mu^2 - m_{\mu\mu,n}^2) - \lambda m_{recoil,n}^2),$$

where κ and λ are determined by fitting the m_{recoil}^2 vs $m_{\mu^+\mu^-}^2$ distribution of the background. The background is a sum of events due to processes which contain a $\mu^+\mu^-$ pair (like $e^+e^- \rightarrow \mu^+\mu^-q\bar{q}$) and events due to fake muons. Monte Carlo generated events are used to evaluate the former background distribution, and real events with isolated $\mu^\pm h^\mp$ or h^+h^- pairs are used for the latter case. The function g_n is a good description of the background distribution, which has limited statistics. Varying κ and λ has little effect on the resulting limits.

The combined factor $\frac{(s f_n + b g_n)}{(s+b)}$ is then the probability distribution for signal plus background. This probability is evaluated for the three events, and the results are multiplied together to get the likelihood.

The 90% C.L. limit of the number of signal events s_{lim} is defined by

$$\frac{\int_0^{s_{lim}} ds \int_0^\infty db \mathcal{L}(s, b)}{\int_0^\infty ds \int_0^\infty db \mathcal{L}(s, b)} = 0.90.$$

FIGURE CAPTIONS

Fig.1 Feynman diagrams of production and decay of the two Higgs bosons.

- (a) Production of a scalar and a pseudoscalar Higgs bosons via a virtual Z .
- (b) Decay of a scalar Higgs boson into a fermion-antifermion pair.
- (c) Decay of a scalar Higgs boson into two pseudoscalar Higgs bosons.
- (d) Decay of a pseudoscalar Higgs boson into a fermion-antifermion pair.
- (e) The main diagram for a background process $e^+e^- \rightarrow \mu^+\mu^-q\bar{q}$ (or $e^+e^- \rightarrow \mu^+\mu^-\tau^+\tau^-$).

Fig.2 Scatter plot of the invariant mass of isolated muon pairs vs squared invariant mass of the recoil particles after cuts (1)-(8). The three surviving events are indicated by crosses. The expected distribution (from Monte Carlo) for $H_i^0H_j^0$ production with $H_j^0 \rightarrow c\bar{c}$ or $\tau^+\tau^-$ and H_i^0 decaying into a muon pair, assuming $M_{H_i^0} = 0.3$ GeV and $M_{H_j^0} = 5$ GeV, is shown in the same figure by dots. The effective luminosity for the simulated Higgs boson events is ten times larger than for the data. The projected distribution onto each axis is also shown.

Fig.3 The limit of the branching fraction for $Z^0 \rightarrow H_p^0H_s^0$ on the Z^0 peak, with all branching fractions 100%, as a function of the heavier Higgs boson mass $M_{H_j^0}$. The Maximum Width curve (dotted curve) is the expected value for $\cos^2(a - b) = 1$.

- (a) $e^+e^- \rightarrow H_i^0H_j^0 \rightarrow \mu^+\mu^- + f\bar{f}$ for $M_{H_i^0} = 0.28$ GeV, just below the $H_i^0 \rightarrow \pi^+\pi^-$ threshold (solid curve), and for $M_{H_i^0} = 0.50$ GeV (dashed curve). $Br(H_i^0 \rightarrow \mu^+\mu^-) = 100\%$
- (b) $e^+e^- \rightarrow H_p^0H_s^0 \rightarrow H_p^0H_p^0H_p^0 \rightarrow \mu^+\mu^- + \mu^+\mu^- + \mu^+\mu^-$ for $M_{H_p^0} = 0.3$ GeV (solid curve) and for $M_{H_p^0} = 0.5$ GeV (dashed curve). $Br(H_s^0 \rightarrow H_p^0H_p^0) = 100\%$ and $Br(H_p^0 \rightarrow \mu^+\mu^-) = 100\%$.

Fig.4 The excluded region in the $M_{H_i^0} - M_{H_j^0}$ plane if branching fractions are 100% and the cross section is maximal (no suppression due to the Higgs mixing).

- (a) $e^+e^- \rightarrow H_i^0 H_j^0 \rightarrow \mu^+\mu^- + f\bar{f}$
- (b) $e^+e^- \rightarrow H_p^0 H_s^0 \rightarrow H_p^0 H_p^0 H_p^0 \rightarrow \mu^+\mu^- + \mu^+\mu^- + \mu^+\mu^-$

REFERENCES

1. G. Altarelli, Proc. of Int. Conf. on High Energy Physics, Berkeley (1986) p119.
2. B.W. Lee, Proc. of Int. Conf. on High Energy Physics, Batavia Illinois (1972) vol.3 p266.
3. H.E. Haber and G.L. Kane, Phys. Reports, 117(1984)279.
4. R.D. Peccei and H.R. Quinn, Phys Rev. Lett., 38(1977)1440;
Phys. Rev., D16(1977)1791
W.A. Bardeen and S.-H.H. Tye, Phys. Lett., 74B(1978)229.
W.A. Bardeen, S.-H.H. Tye and J.A.M. Vermaseren, Phys. Lett., 76B(1978)580.
5. H.E. Haber, G.L. Kane and T. Sterling, Nucl. Phys. B161(1979)493
Phys. Rev., D16(1977)1791.
6. J.F. Gunion and H.E. Haber, Nucl. Phys. B272(1986)1.
7. G. Pocsik and G. Zsigmond, Z. Physik, C10(1981)367.
8. H. Baer et al., edited by J. Ellis and R.D. Peccei, CERN 86-02(1986)340.
9. S. Glashow and S. Weinberg, Phys. Rev. D15(1977)1958.
10. L.F. Abbott, P. Sikivie and M.B. Weiss, Phys. Rev. D21(1980)1393.
11. Ying Liu, Z. Physik, C30(1986)631.
12. CLEO Collab., P. Avery et al., contributed paper for the Int. Conf. on Lepton and Photon Int. at High Energies at Hamburg (1987).
13. R.S. Chivukula and A. Manohar, Phys. Lett. B207(1988)86.
14. CUSB Collab., J. Lee-Franzini, to be seen in the Proc. of the Int. Conf. on High Energy Physics, Munich, 1988.
15. S.L. Glashow and A. Manohar, Phys. Rev. Lett., 54(1985)526.

16. UA1 Collab., G. Arnison et al., Phys. Lett., 139B(1984)115.
17. HRS Collab., C. Akerlof et al., Phys. Lett., 156B(1985)271.
18. MAC Collab., W.W. Ash et al., Phys. Rev. Lett., 54(1985)2477.
19. Mark-II Collab., G.J. Feldman et al., Phys. Rev. Lett., 54(1985)2289.
20. CELLO Collab., H.J. Behrend et al., Phys. Lett., 161B(1985)18.
21. JADE Collab., W. Bartel et al., Phys. Lett., 155B(1985)288, and updated result is in Ref.22.
22. K. Hagiwara and S. Komamiya, KEK-TH 145, to appear in the High Energy Electron-Positron Physics, edited by A. Ali and P. Soding, World Scientific.
23. R.D. Peccei, T.T. Wu and T. Yanagida, Phys. Lett., B172(1986)435.
24. L.M. Krauss and F. Wilczek, Phys. Lett., B173(1986)189.
25. T. Cowan et al., Phys. Rev. Lett., 56(1986)446.
26. K. Hagiwara, DESY/KEK, private communication.
27. S. Egli et al., SIN preprint, PR-86-08 (1986).
28. A. Konaka et al., Phys. Rev. Lett. 57(1986)659
C.N. Brown et al., Phys. Rev. Lett. 57(1986)2101.
29. M.B. Voloshin, Sov. J. Nucl. Phys. 44(1986)478;
S. Raby and G.B. West, contributed paper No. 501 for the Int. Conf. on High Energy Physics, Munich 1988.
30. H.E. Haber, private communication.
31. R.H. Schindler et al., Phys. Rev. D 24(1981)78.
32. G.S. Abrams et al., IEEE Trans. Nucl. Sci. NS25(1978)309
G.S. Abrams et al., IEEE Trans. Nucl. Sci. NS27(1980)59.
33. G.S. Abrams et al., SLAC-PUB-4558(1989).

34. G. Hanson, Nucl. Instr. and Meth. A252(1986)343.
35. W.T. Ford *et al.*, Nucl. Instr. and Meth. A255(1987)480.
36. R.C. Jared *et al.*, I.E.E.E. Trans. Nucl. Sci. N-S33(1986)916.
37. M.E. Nelson *et al.*, Phys. Rev. Lett. 50(1983)1542.
38. F.A. Berends, P.H. Daverveldt and R. Kleiss, Phys. Lett. 148B(1984)489;
Nucl. Phys. B253(1985)441.
39. R.A. Ong, thesis, SLAC-320 (1988).

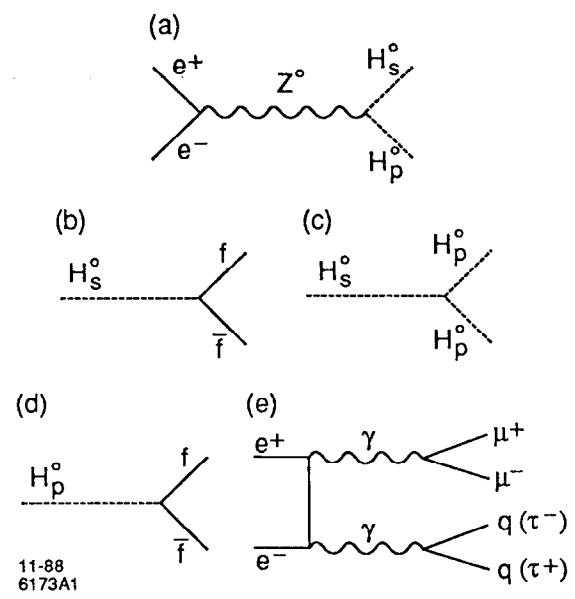


Fig. 1

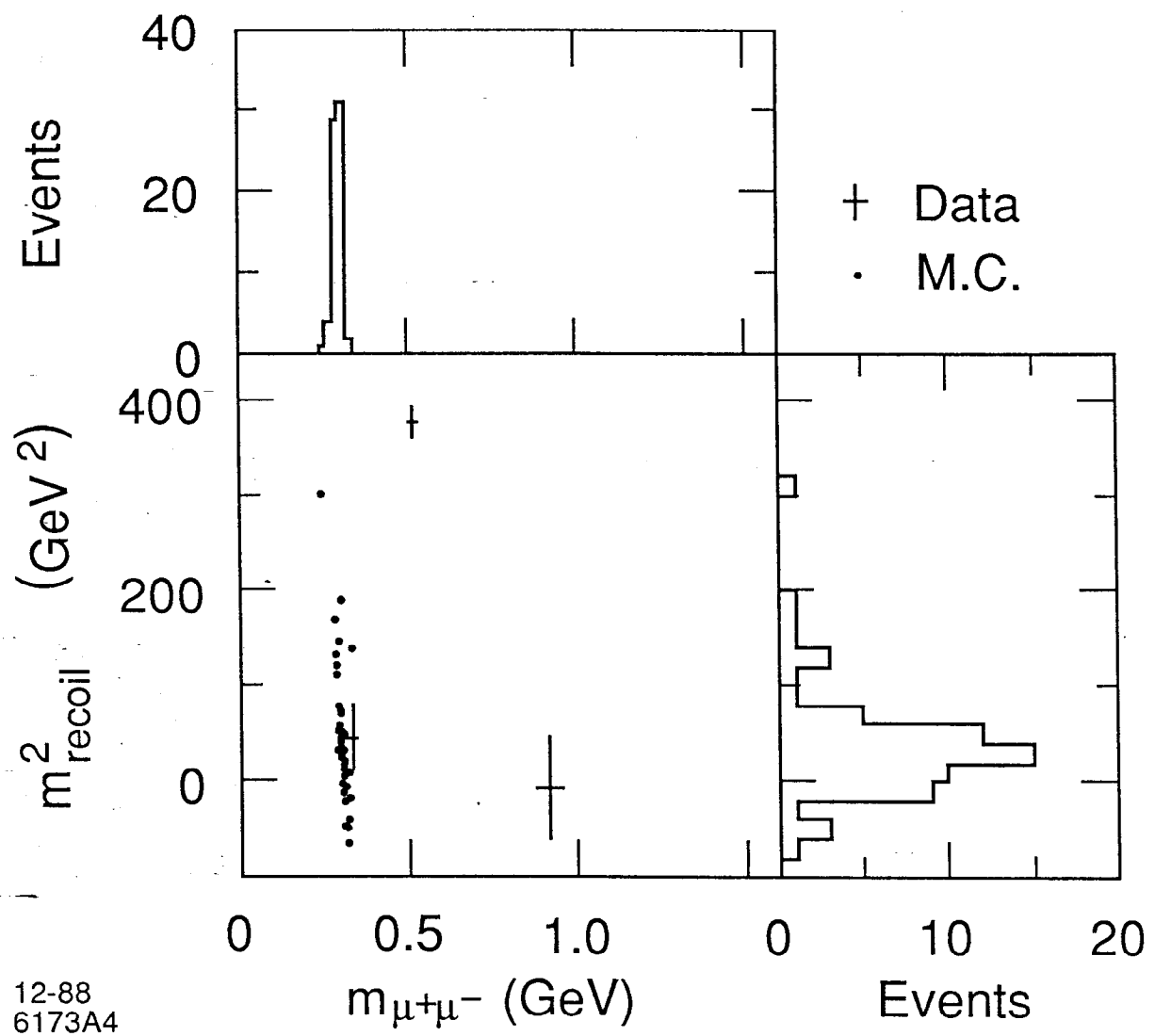


Fig. 2

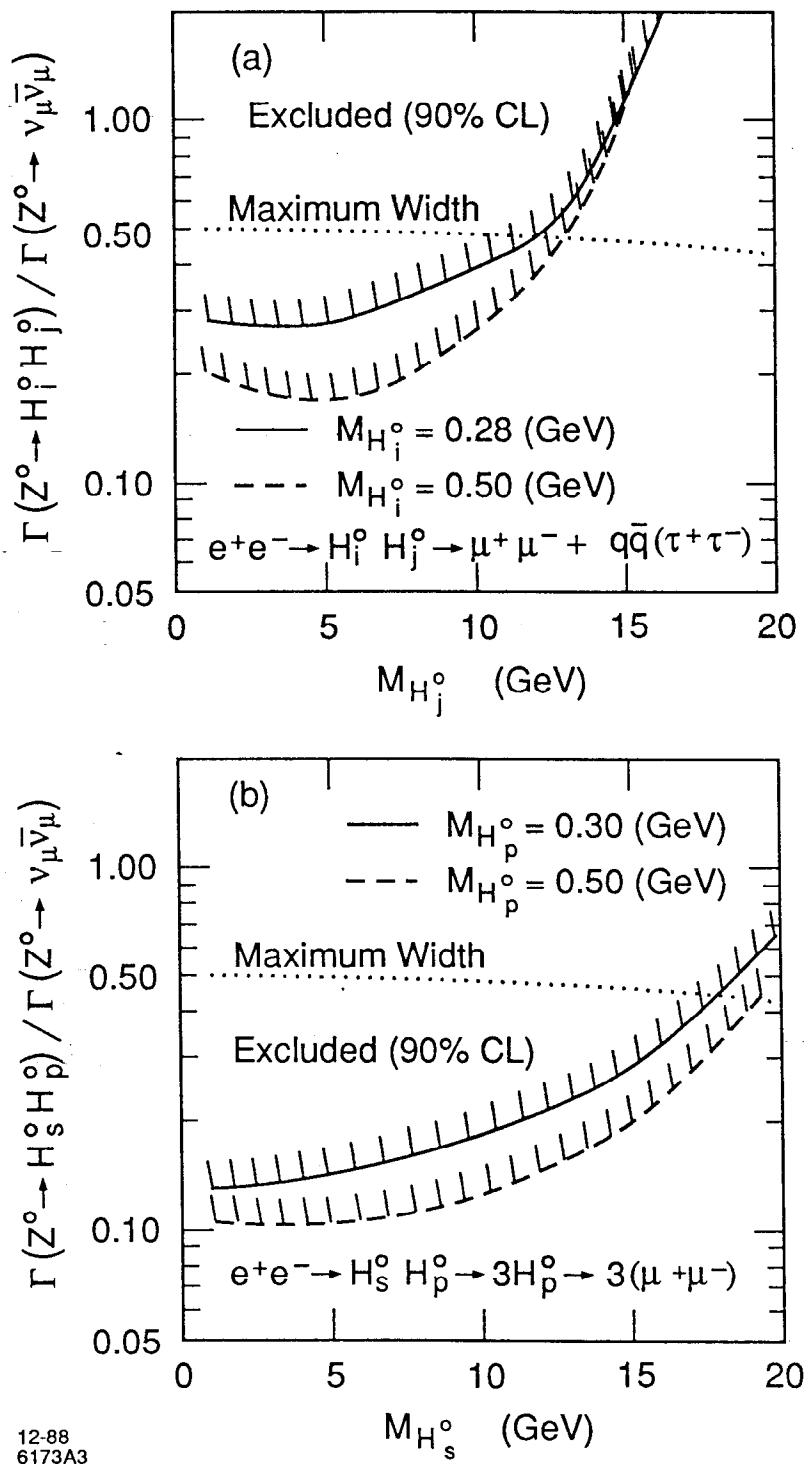


Fig. 3

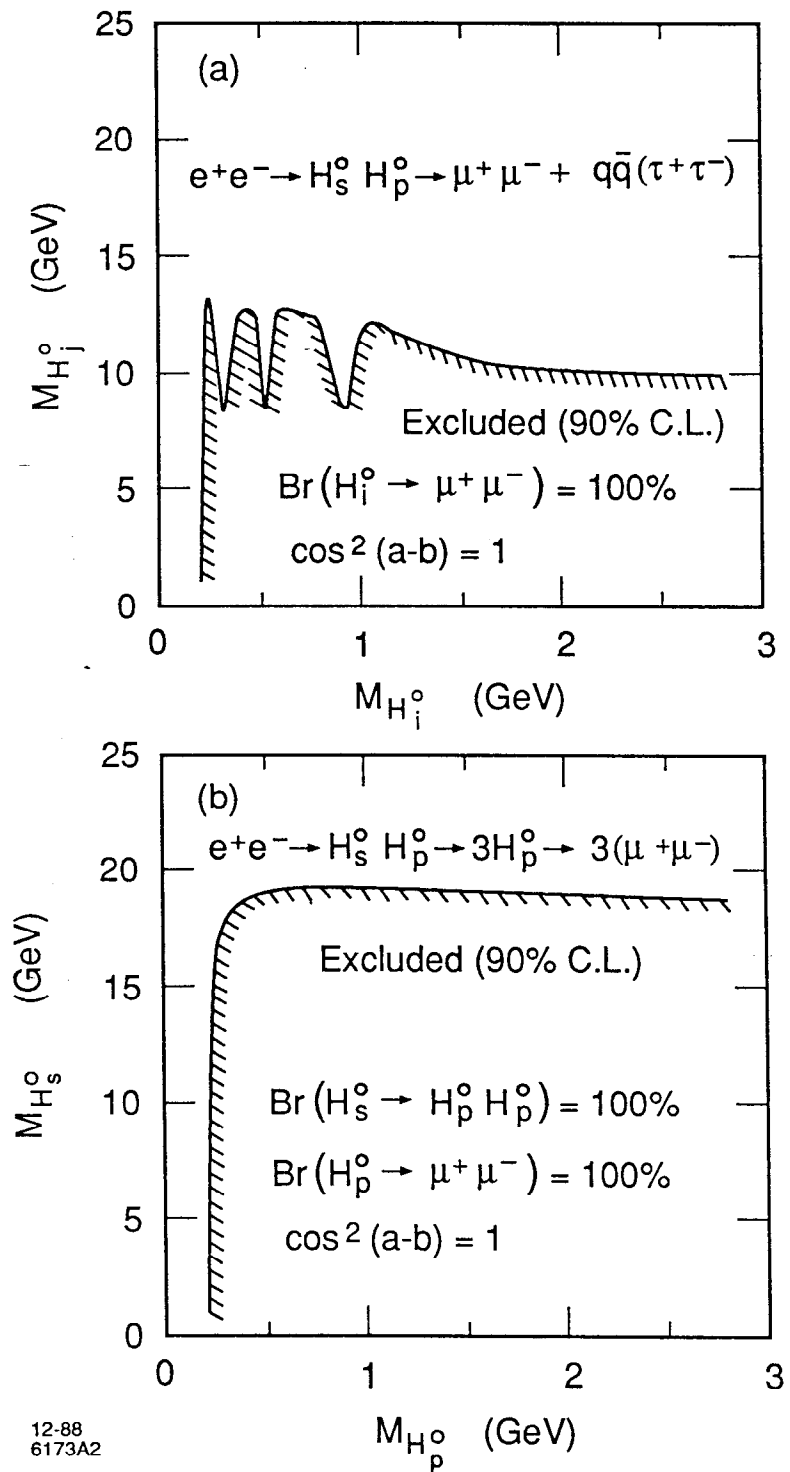


Fig. 4